Theoretical Modeling and Energy Conversion Process of Free Piston Internal Combustion Power System

Limin Wu, Huihua Feng✉, Ziwei Zhang, Yao Wang, Boru Jia and Xiaodong Yan
(School of Mechanical Engineering, Beijing Institute of Technology, Beijing 100081, China)

Abstract: A numerical model for energy flow calculation of the free piston internal combustion power system (FPICPS) was established, which was compared with the traditional internal combustion engine (IC engine) with the same structure and input conditions. The piston motion characteristics and energy transfer process of FPICPS are studied by numerical simulation method. The results show that the changes of cylinder pressure, temperature and piston motion characteristics of free piston engine (FP engine) lag behind those of IC engine, and the piston peak acceleration of the FP engine is approximately 2.8 times that of IC engine. The proportion of compression stroke and expansion stroke of IC engine is basically the same, while the expansion stroke of FP engine only accounts for 41.6% of the whole operating cycle. FP engine have obvious advantages in heat transfer and air leakage loss, their percentages are 11.82% and 0.83%, respectively. The percentage of indicated power in FP engine and IC engine are 27.44% and 25.98%, respectively. And 79.64% of FP engine indicated power is converted into the motor electromagnetic energy.

Key words: free piston internal combustion power system (FPICPS); numerical model; kinematic characteristics; energy conversion process

CLC number: TK441.1 **Document code:** A **Article ID:** 1004-0579(2021)S1-0035-09

The free piston internal combustion power system (FPICPS) is formed by coupling a free piston (FP) engine and a linear motor, it can convert the kinetic energy of the free piston directly into the electric energy of the linear motor. It potentially carries the advantages of compact structure, low vibration and noise level, and rapid transient response, which has attracted extensive attention of researchers[1].

There are various forms of FPICPS, researchers have done a lot of simulation studies on different types of FPICPS[2-7]. Mao Jinlong[2] established a free piston generator numerical model and conducted a preliminary analysis of its performance. Tian Chunlai et al.[3] transformed a single-cylinder free piston generator to a single degree of freedom self-excited oscillation system, so as to design and optimize the system. Jaeheun Kim[4] et al. analyzed the combustion process in the free piston engine cylinder based on the Webie function, and studied the effects of combustion duration and ignition timing on piston dynamics and engine performance; Boru Jia[5] et al. established a numerical simulation model for the start-up process and stable operation of a spark-ignition free piston generator, and verified the accuracy of the simulation model experimentally. Chendong Guo[7] et al. used the simulation model to analyze the dual-piston free-piston internal combustion engine. Parameter analysis was carried out to obtain the operating characteristics of the piston under power generation conditions.

Received 2020-10-20
Supported by the National Natural Science Foundation of China (51675043)
✉ Author for correspondence, professor, Ph.D.
E-mail: fenghh@bit.edu.cn
DOI: 10.15918/j.jbit1004-0579.20112

Many researchers have compared the piston motion characteristics of a FP engine with those of the internal combustion (IC) engine[8-16]. Researchers have found that, the piston speed of an FP engine changes more violently near the top center than that of an IC engine, that is, the acceleration value is larger[8-16]. In addition, A.P. Roskilly[8, 10, 11] and Shuaiqing Xu[13] et al. found that the moment in time which the piston reaches the TDC in a free-piston engine was slightly later than the IC engine.

Researchers have done a lot of comparative analyses on the piston motion characteristics of the FP engine and IC engine. However, researchers have seldom analyzed the energy flow during the operation cycle of the FPICPS, and the property of energy flow is still unclear. Therefore, it is necessary to compare and analyze the energy transfer process between the FPICPS and the IC engine.

The piston dynamics and thermal process in the cylinder of an FPICPS and IC engine are respectively modeled under the same engine structure parameters. The cylinder temperature, the cylinder pressure, the piston motion characteristics and the energy transfer process are compared.

1 Numerical Model of FPICPS

The FPICPS is shown in Fig. 1. The system consists of a FP engine, a linear motor, and a rebound device. The engine adopts the form of two-stroke and uniflow scavenging. The scavenging and exhaust timing are controlled by the piston motion. The linear motor is a three-phase permanent magnet synchronous motor, and the motor is a permanent magnet, and the stator interior is a three-phase winding. The rebound cylinder is composed of a cylinder block and the rebound piston. The air is supplied to the cylinder by the external controllable flow air source. The main design specifications for the engine are listed in Tab. 1

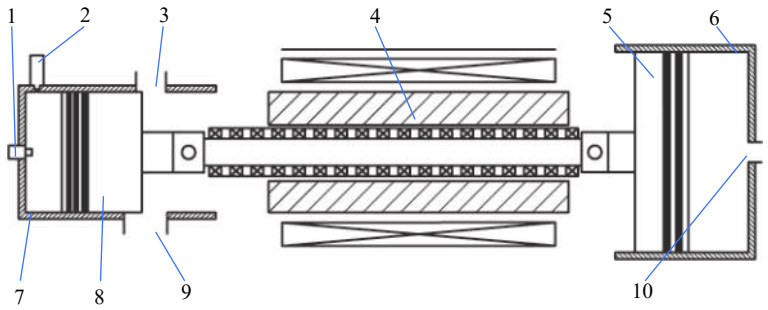

1-Sparking plug; 2-Fuel injector; 3-Scavenging port; 4-Linear motor; 5-Rebound piston; 6-Rebound cylinder; 7-Engine block; 8-Engine piston; 9-Exhaust port; 10-Rebound cylinder air port

Fig. 1 Schematic of FPICPS

Tab. 1 Engine specifications

Engine type	Scavenging arrangements	Compression ratio	Stroke	Bore/mm	Stroke/mm	Rated speed/(r·min^{-1})
Gasoline engine	Uniflow scavenging	10	Two stroke	56.5	56.5	2.85%

1.1 Dynamic model of FP engine mover

In the FPICPS, the engine piston, the linear motor rotor and the rebound piston are connected as one unit, which is called a mover. There are no mechanical constraints on the mover, and its motion is completely determined by the external force, and the force is shown in Fig. 2.

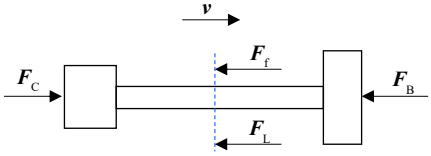

Fig. 2 Free body diagram of FP engine mover

According to the Newton's 2nd law, the motion of the mover can be described as

$$\boldsymbol{F}_{\mathrm{B}}+\boldsymbol{F}_{\mathrm{C}}+\boldsymbol{F}_{\mathrm{f}}+\boldsymbol{F}_{\mathrm{L}}=m_{\mathrm{R}}\frac{\mathrm{d}^{2}\boldsymbol{x}}{\mathrm{d}t^{2}} \tag{1}$$

where m_{R} is the mass of the mover and $\boldsymbol{x}$ is its position, $\boldsymbol{F}_{\mathrm{B}}$ is the rebound cylinder pressure force, $\boldsymbol{F}_{\mathrm{C}}$ is the engine cylinder pressure force, $\boldsymbol{F}_{\mathrm{f}}$ is the friction force of the mover, and $\boldsymbol{F}_{\mathrm{L}}$ is the force acted by the linear motor.

The cylinder pressure force is equal to the pressure in the cylinder times the area of the piston top area

$$\boldsymbol{F}_{\mathrm{B}}=\boldsymbol{p}_{\mathrm{B}}A_{\mathrm{B}} \tag{2}$$

$$\boldsymbol{F}_{\mathrm{C}}=\boldsymbol{p}_{\mathrm{C}}A_{\mathrm{C}} \tag{3}$$

where $\boldsymbol{p}_{\mathrm{B}}$ is rebound cylinder pressure, $\boldsymbol{p}_{\mathrm{C}}$ is engine cylinder pressure, A_{B} is rebound piston top area, and A_{C} is engine piston top area.

1.2 Friction force of FP engine mover

The mover motion frequency of FPICPS is relatively low, so the contact parts of the mover are well lubricated[17]. In order to simplify the modeling process and improve the calculation efficiency, the friction force on the mover can be described as Ref. [18]

$$\boldsymbol{F}_{\mathrm{f}}=-k_{\mathrm{f}}\boldsymbol{v} \tag{4}$$

where k_{f} is the friction coefficient, $\boldsymbol{v}$ is the speed of the mover.

1.3 Numerical model of electromagnetic force in linear motor

The motor has various forms and different characteristics. It is found that the electromagnetic force has a positive proportion with the current and the moving speed of the mover, such as Ref. [19]

$$\boldsymbol{F}_{\mathrm{L}}=K_{\mathrm{L}}\frac{\mathrm{d}\boldsymbol{x}}{\mathrm{d}t} \tag{5}$$

$$\boldsymbol{F}_{\mathrm{L}}=K_{i}I \tag{6}$$

where K_{L} is the load coefficient of the motor ($\mathrm{N/m\cdot s^{-1}}$), K_i is the thrust coefficient of linear motor ($\mathrm{N/A}$), when the motor structure is determined, the two coefficients are determined accordingly. Eq. (5) is used in the numerical model to connect the displacement of the mover with the electromagnetic force.

1.4 Thermodynamic model in engine cylinder

To describe the state of the mixture in the cylinder, a thermal system is specified. The boundary of the system consists of the piston top, the cylinder head and the cylinder liner surface. In particularly, assume that the state of the mixture in the cylinder is uniform, the mixture is an ideal gas, and the process of gas flowing into or out of the cylinder is a quasi-steady flow process, and assume that the gas leakage area is constant.

① The ideal gas state equation

By considering that the mixture in the cylinder is an ideal gas, and then at any instant the ideal gas state equation is satisfied.

$$pV=mR_{\mathrm{g}}T \tag{7}$$

② Mass conservation equation

According to the principle of mass conservation

$$\frac{\mathrm{d}m}{\mathrm{d}t}=\frac{\mathrm{d}m_{\mathrm{air}}}{\mathrm{d}t}-\frac{\mathrm{d}m_{\mathrm{ex}}}{\mathrm{d}t}+\frac{\mathrm{d}m_{\mathrm{b}}}{\mathrm{d}t}-\frac{\mathrm{d}m_{\mathrm{l}}}{\mathrm{d}t} \tag{8}$$

where m_{air} is the mass of air flow into the cylinder, m_{ex} is the mass of exhaust gas, m_{b} is the mass of burned fuel, and m_{l} is the mass leaking from piston rings.

When the fuel injection quantity of the engine is m_{fc} and the fuel combustion percentage in the cylinder is $\eta_{\mathrm{fu}}=m_{\mathrm{b}}/m_{\mathrm{fc}}$, then

$$\frac{\mathrm{d}m_{\mathrm{b}}}{\mathrm{d}t}=m_{\mathrm{fc}}\frac{\mathrm{d}\eta_{\mathrm{fu}}}{\mathrm{d}t} \tag{9}$$

According to Eq. (9), the rate of change in heat released by fuel combustion is

$$\frac{\mathrm{d}Q_{\mathrm{b}}}{\mathrm{d}t}=m_{\mathrm{fc}}\frac{\mathrm{d}\eta_{\mathrm{fu}}}{\mathrm{d}t}H_{\mathrm{u}}\eta_{\mathrm{u}} \tag{10}$$

Consequently, the conservation of mass equation can be written as

$$\frac{\mathrm{d}m}{\mathrm{d}t}=\frac{\mathrm{d}m_{\mathrm{air}}}{\mathrm{d}t}-\frac{\mathrm{d}m_{\mathrm{ex}}}{\mathrm{d}t}+m_{\mathrm{fc}}\frac{\mathrm{d}\eta_{\mathrm{fu}}}{\mathrm{d}t}+\frac{\mathrm{d}m_{\mathrm{l}}}{\mathrm{d}t} \tag{11}$$

③ Energy conservation equation

According to the first law of thermodynamics, there are

$$\frac{\mathrm{d}U}{\mathrm{d}t}=\frac{\mathrm{d}Q_{\mathrm{b}}}{\mathrm{d}t}+\frac{\mathrm{d}m_{\mathrm{air}}}{\mathrm{d}t}h_{\mathrm{air}}-\frac{\mathrm{d}m_{\mathrm{ex}}}{\mathrm{d}t}h_{\mathrm{ex}}-\frac{\mathrm{d}m_{\mathrm{l}}}{\mathrm{d}t}h_{\mathrm{l}}-\frac{\mathrm{d}Q_{\mathrm{t}}}{\mathrm{d}t}-p\frac{\mathrm{d}V}{\mathrm{d}t} \tag{12}$$

where U is the internal energy of the mixture, Q_{b} is the heat release from fuel combustion, m_{air} is the mass of air flow into the cylinder, h_{air} is the increased enthalpy of air flowing into the cylinder, m_{ex} is the mass of air exhaust from the cylinder, h_{ex} is the decreased enthalpy of air exhaust from the cylinder, m_{l} is the mass of air leaking through the piston rings, h_{l} is the decreased enthalpy of air leaking through the piston rings, Q_{t} is the heat exchange between the mixture and cylinder, p is the cylinder pressure, V is the cylinder instantaneous volume.

According to the definition of internal energy, we have

$$\frac{\mathrm{d}U}{\mathrm{d}t}=\frac{\mathrm{d}(mu)}{\mathrm{d}t}=u\frac{\mathrm{d}m}{\mathrm{d}t}+m\frac{\mathrm{d}u}{\mathrm{d}t} \tag{13}$$

and the specific internal energy can be simplified as a function of temperature and generalized excess air coefficient

$$u=u(T,\alpha_x) \tag{14}$$

where u is the specific internal energy, T is temperature, α_x is the generalized excess air coefficient.

By substituting Eq. (14) into Eq. (13), we have

$$\frac{\mathrm{d}U}{\mathrm{d}t}=\frac{\mathrm{d}(mu)}{\mathrm{d}t}=u\frac{\mathrm{d}m}{\mathrm{d}t}+m\left(\frac{\partial u}{\partial T}\frac{\mathrm{d}T}{\mathrm{d}t}+\frac{\partial u}{\partial\alpha_{\mathrm{x}}}\frac{\mathrm{d}\alpha_{\mathrm{x}}}{\mathrm{d}t}\right)=u\frac{\mathrm{d}m}{\mathrm{d}t}+m\left(c_{\mathrm{V}}\frac{\mathrm{d}T}{\mathrm{d}t}+\frac{\partial u}{\partial\alpha_{\mathrm{x}}}\frac{\mathrm{d}\alpha_{\mathrm{x}}}{\mathrm{d}t}\right) \tag{15}$$

where $\frac{\partial u}{\partial T}|_{V=C}=c_{\mathrm{V}}$, C is constant.

By substituting Eq. (15) into Eq. (12), we have

$$\frac{\mathrm{d}T}{\mathrm{d}t}=\frac{1}{mc_{\mathrm{V}}}\left(\frac{\mathrm{d}Q_{\mathrm{b}}}{\mathrm{d}t}+\frac{\mathrm{d}m_{\mathrm{air}}}{\mathrm{d}t}h_{\mathrm{air}}-\frac{\mathrm{d}m_{\mathrm{ex}}}{\mathrm{d}t}h_{\mathrm{ex}}-\frac{\mathrm{d}m_{\mathrm{l}}}{\mathrm{d}t}h_{\mathrm{l}}-\frac{\mathrm{d}Q_{\mathrm{t}}}{\mathrm{d}t}-p\frac{\mathrm{d}V}{\mathrm{d}t}-u\frac{\mathrm{d}m}{\mathrm{d}t}-m\frac{\partial u}{\partial\alpha_{\mathrm{x}}}\frac{\mathrm{d}\alpha_{\mathrm{x}}}{\mathrm{d}t}\right) \tag{16}$$

The temperature increment can be calculated by Eq.(16), and the cylinder pressure can be calculated from Eq. (7).

1.5 Thermodynamic model in rebound cylinder

Compared to the working process in the engine cylinder, the combustion process does not occur in rebound cylinder, and the calculation of thermodynamic process in cylinder is as follows.

$$\frac{\mathrm{d}T}{\mathrm{d}t}=\frac{1}{mc_{\mathrm{V}}}\left(\frac{\mathrm{d}m_{\mathrm{in}}}{\mathrm{d}t}h_{\mathrm{in}}-\frac{\mathrm{d}m_{\mathrm{l}}}{\mathrm{d}t}h_{\mathrm{l}}-\frac{\mathrm{d}Q_{\mathrm{t}}}{\mathrm{d}t}-p\frac{\mathrm{d}V}{\mathrm{d}t}-u\frac{\mathrm{d}m}{\mathrm{d}t}\right) \tag{17}$$

where the definition of each variable is the same as that in the engine cylinder, so it will not be repeated here.

2 Comparative Analyses of Energy Transfer Process Between FPICPS and IC Engine

2.1 Equivalent conversion method of piston motion

In this paper, the piston motion of a traditional engine is transformed into reciprocating linear motion in the time domain by equivalent transformation. The piston motion profile is applied to the piston of FPICPS, and the running process of the FPICPS and the IC engine is compared.

Structure of traditional IC engine is shown in Fig. 3, the position of piston is

$$x=R/\lambda+R-R\cos\alpha-\sqrt{(R/\lambda)^2-(R\sin\alpha)^2} \tag{18}$$

where R is the crank radius, L is the connecting rod length, α is the angle between the crank and the cylinder axis, and the connecting rod ratio is $\lambda=R/L$, the values range is from 1/4 to 1/3, in this paper, we used 1/3.

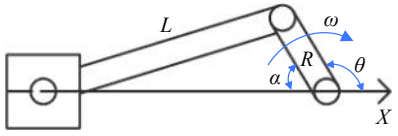

Fig. 3 Structure of IC engine

The crankshaft of IC engine is equipped with a flywheel, which causes the crankshaft to rotate almost uniformly, therefore it holds that

$$\theta = \omega t \tag{19}$$

where θ is the positive angle between the crank and x axis, and ω is the angular velocity of the crank rotation.

Thus, we have the following relationship as

$$\begin{cases} \alpha + \theta = (2n+1)\pi, \\ \quad 2n\pi \le \theta < (2n+1)\pi, n \in N \\ \theta - \alpha = (2n+1)\pi, \\ \quad (2n+1)\pi \le \theta < (2n+2)\,\pi, n \in N \end{cases} \tag{20}$$

2.2 Kinematic results analyses

The cylinder temperature and pressure of FP engine and IC engine are obtained via numerical calculation, as shown in Fig. 4.

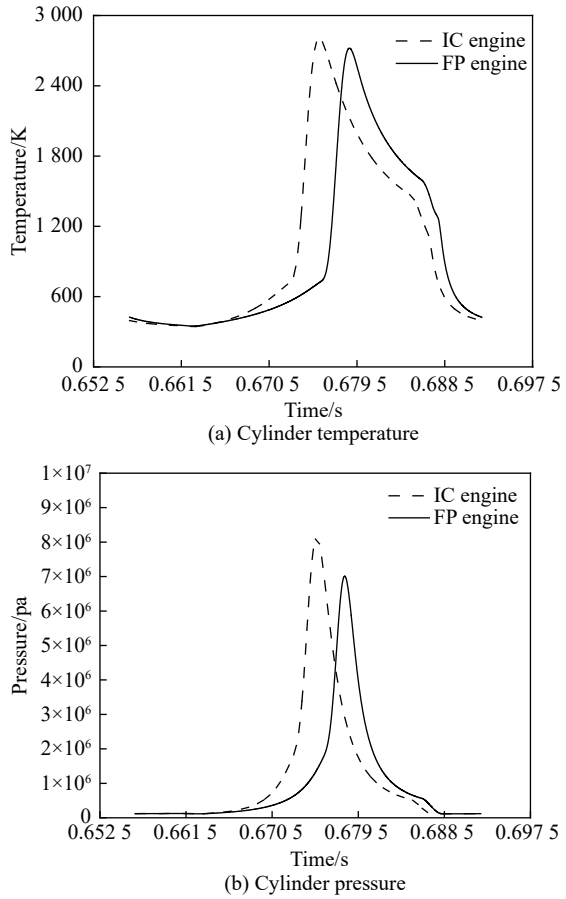

Fig. 4 Cylinder temperature and pressure of IC engine and FP engine

It can be seen from Fig. 4a and Fig.4b that the temperature in the cylinder of the IC engine rises ahead of time, thus the cylinder pressure rises in advance. The peak temperature of the FP engine and IC engine are 2 721 K and 2 805 K, respectively. The peak cylinder pressure of the FP engine and IC engine are 7.013 MPa and 8.143 MPa, respectively. It is apparent that the FP engine operate in less harsh conditions than the IC engine. There exists a short-term fluctuation in the decreasing stage of cylinder temperature and pressure. In this stage, the piston speed increases significantly in the expansion stroke. When the piston moves to a certain distance, the exhaust port and the scavenging port successively open, causing a lot of heat to be discharged.

The temperature and pressure are closely related to the thermodynamic processes in the cylinder and can directly affect the piston motion characteristics. Fig. 5a shows the piston acceleration. The peak acceleration of the piston in the FP engine is 2 791 m/s^2, which is about 2.8 times of the IC engine, and the accelerations are obviously different. The movement of IC engine piston is restrained by the crank connecting rod mechanism. However, in the free piston engine, there is no mechanical constraint on the piston, and the conversion of kinetic energy and magnetic energy near the dead center almost stops, so the peak acceleration of FP engine is relatively large.

The velocity and displacement in Fig. 5a - 5b show that the piston speed and duration of compression stroke are almost the same as expansion stroke in the IC engine. However, the piston speed of the FP engine during the compression stroke is apparently smaller than the expansion stroke, and the proportion of expansion stroke duration is only 41.6%, it is beneficial to reduce the heat transfer loss and improve the conversion efficiency.

Furthermore, the piston motion characteristics shown in Fig. 5 are consistent with the results in Refs. [8, 10, 11, 13] which have been verified by previous experiments. It is proven that the simulation model established in this paper is accurate.

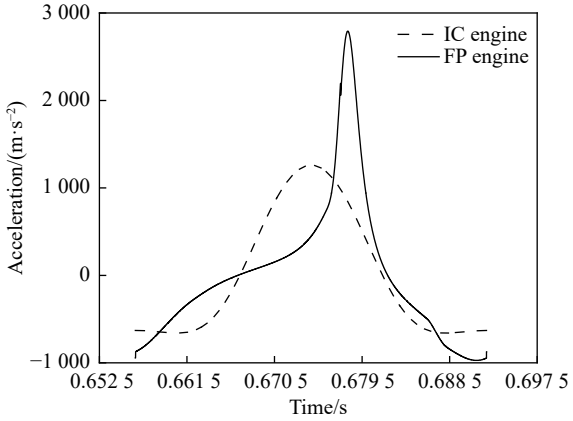

(a) Piston acceleration of IC engine and FP engine

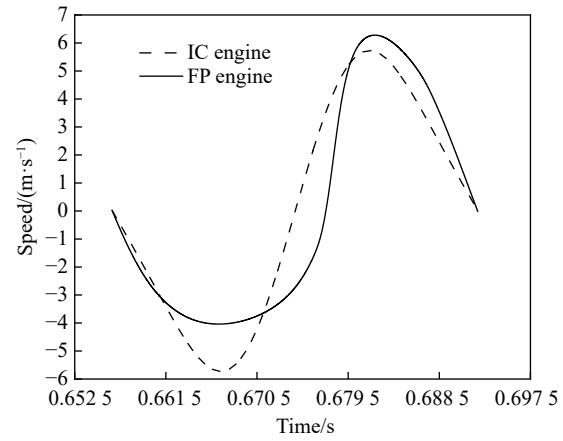

(b) Piston speed of IC engine and FP engine

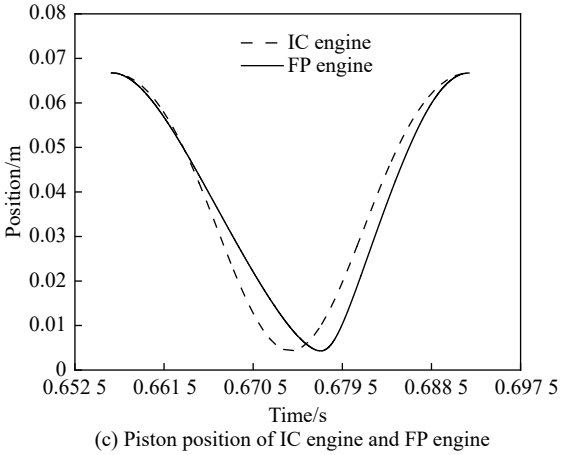

(c) Piston position of IC engine and FP engine

Fig. 5 Comparison of piston motion characteristics between IC engine and FP engine

2.3 Comparative analyses of thermodynamic process in engine cylinder

Fig. 6 shows the comparison of cylinder temperature, combustion heat release and pressure rise rate. The peak pressure rise rate of the FP engine is lower than that of the IC engine, and the peak value time of FP engine is later than that of the IC engine. The reason for this phenomenon is that at the same ignition position, the FP engine piston moves at a slower speed in the compression stroke, and the piston ignition time is delayed, thus delaying the combustion. The heat release curve of the FP engine is delayed for the same reason. As shown in the enlarged area in the figure, the exhaust port and scavenging port are opened successively, resulting in the change of the input energy and mass in the cylinder, and make the pressure rise rate fluctuate obviously, which in turn affects the piston motion characteristics and ultimately affects the system efficiency.

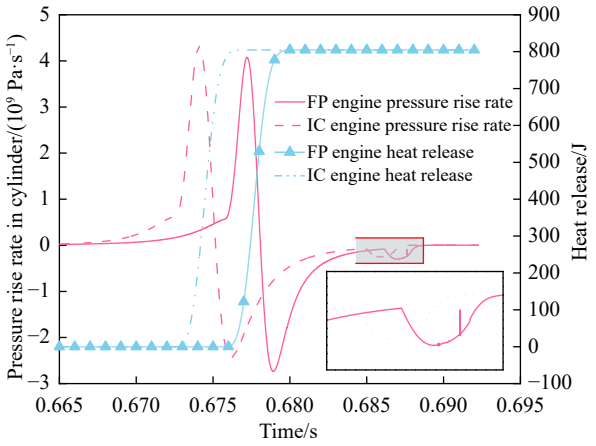

Fig. 6 Comparison of cylinder temperature, combustion heat release and pressure rise rate

Fig. 7 shows the comparative analysis of different stages of combustion. In Fig. 7, *a*-*b* and *a*′-*b*′ corresponds to the ignition pulse widths, *b*-*c* and *b*′-*c*′ are the ignition delay period, *c*-*d* and *c*′-*d*′ are the rapid burning period, and *d*-*e* and *d*′-*e*′ represents the post burning period. Although the pulse widths of *a*-*b* and *a*′-*b*′ are the same, the piston of the IC engine moves faster in the compression stroke, the ignition signal is triggered first, and the cylinder pressure is higher than FP engine when the spark plug starts ignition, so the ignition delay period of IC engine is shorter than that of the FP engine.

Fig. 8 shows the proportion of different stages in the combustion processes of IC engine and FP engine. As mentioned above, the igni-

tion delay period of the FP engine is longer than that of the IC engine, accounting for 48.91% of the whole combustion cycle, while the proportion of the rapid burning period and the post burning period of FP engine are lower than those of IC engine, which are 29.37% and 21.71% respectively. Compared to the dual cylinder dual piston free piston internal combustion power system developed by our research group, the post burning period is significantly reduced, which is mainly due to the improvement of the single cylinder structural stiffness. Therefore, in terms of combustion, it is necessary to improve the system structure and the piston motion control method.

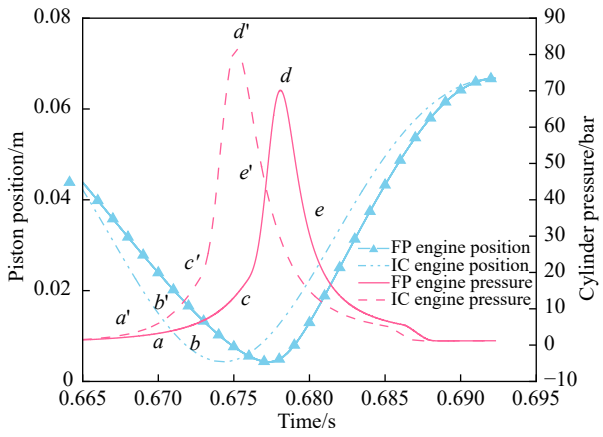

Fig. 7 Comparative analyses of different combustion stages

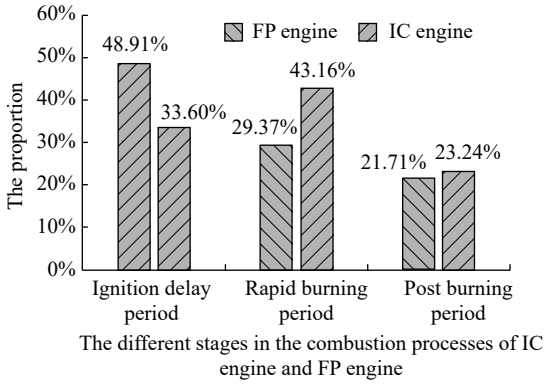

Fig. 8 Comparative analyses of different combustion stage proportion

2.4 Comparative analyses of energy conversion process

The FP engine, linear motor and rebound device operate synergistically in FPICPS to realize the conversion and transfer of chemical energy to magnetic energy[18]. In the operating cycle, Eq. (16) can be used to analyze the energy conversion and transfer process according to the law of conservation of energy. The energy output of the FPICPS is different from that of the traditional IC engine, while the energy conversion process from chemical energy to piston kinetic energy is the same. Furthermore, for the FPICPS, the energy conversion from kinetic energy to electromagnetic energy needs to be analyzed.

As can be seen from Tab. 2, the proportion of heat energy released by fuel combustion of FP engine (63.22%) is higher than that of the IC engine (62.21%), but the energy imported with air into the engine cylinder is lower (27.3%). The exhaust loss of the FP engine is 55.37%, which is higher than that of IC engine. FP engines have improved metrics of heat transfer loss and air leakage loss, which are 11.82% and 0.83%, respectively, while the heat transfer loss and air leakage loss of IC engine are 14.52% and 1.08%, respectively. Furthermore, the proportion of indicated power of the FP engine is higher than that of the IC engine, which is 27.44%, And

Tab. 2 Energy conversion and distribution diagram within a single cycle of FPICPS and IC engine

The percentage of energy that inputs into the system			
Type	*A*/%	*B*/%	*C*/%
FPICPS	63.22	27.30	9.47
IC engine	62.21	29.87	7.92

Various parts of energy transformed and transmitted through the system					
Type	*D*/%	*E*/%	*F*/%	*G*/%	*H*/%
FPICPS	55.37	27.44	11.82	0.83	4.54
IC engine	54.68	25.98	14.52	1.08	3.74

Conversion of piston kinetic energy in FPICPS			
Type	*I*/%	*J*/%	*K*/%
FPICPS	79.64	17.61	2.85

A- Heat energy released by fuel combustion; *B*- Energy imported with air into the engine cylinder; *C*- The increased internal energy due to changes of the mixture mass in the cylinder; *D*- Exhaust loss; *E*- Kinetic energy transferred to the piston; *F*- Heat transfer loss; *G*- Leakage loss; *H*- Energy fluctuation loss; *I*- Electromagnetic energy of the motor; *J*- Friction loss; *K*- Work on rebound cylinder.

79.64% of the FP engine indicated power is converted into the motor electromagnetic energy.

The FPICPS has obvious advantages in terms of combustion heat release, heat transfer loss and air leakage loss due to its unique motion characteristics and structural characteristics. Furthermore, the system efficiency can be further improved by optimizing the intake and exhaust process and also reducing the system friction. Therefore, the analysis of the energy conversion of the system can indicate the direction of system improvement to a certain extent.

3 Conclusions

Through the comparative analyses of the FPICPS and the IC engine, the following conclusions are drawn as follows.

① In the compression stroke of the IC engine, the piston moves faster, which triggers the ignition signal in advance and makes the mixture in the cylinder burn ahead of time, subsequently raising the temperature and pressure in the cylinder in advance.

② The peak temperature and pressure of the FP engine are 2721 K and 7.013 MPa respectively, which are lower than those of the IC engine. The results show that the working conditions of the FP engine are smoother than those of the IC engine.

③ Under the same ignition position and pulse width, the piston speed of the FP engine in compression stroke is slow, and the time to the reach ignition position is delayed, which results in the combustion delay, and consequently the delay in heat release. The opening of the exhaust port and scavenging port successively lead to the change in the input energy and mass in the cylinder, which makes the pressure rise rate fluctuate significantly.

④ The ignition delay period of free piston engine accounts for 48.91% of the whole combustion cycle, which is longer than that of a traditional engine, while the proportion of the rapid burning period and the post burning period are 29.37% and 21.71%, respectively, which are lower than those of a traditional engine.

⑤ The FP engine has obvious advantages in heat transfer loss and air leakage loss . The heat transfer loss and air leakage loss are 11.82% and 0.83% respectively, while the heat transfer loss and air leakage loss of IC engine are 14.52% and 1.08% respectively. Furthermore, the proportion of indicated power of the FP engine is higher than that of the IC engine, which is 27.44%. Additionally, 79.64% of the FP engine indicated power is converted into the motor electromagnetic energy.

References:

[1] Mikalsen R, Roskilly A P. A review of free-piston engine history and applications [J]. Applied Thermal Engineering, 2007, 27(14-15): 2339-2352.

[2] Mao Jinlong, Zuo Zhengxing, Liu Dong. Numerical simulation of a spark ignited two-stroke free-piston engine generator [J]. Journal of Beijing Institute of Technology, 2009, 18(3): 283-287.

[3] Tian Chunlai, Feng Huihua, Zuo Zhengxing. Oscillation characteristic of single free piston engine generator [J]. Advanced Materials Research, 2011, 383-390: 1873-1878.

[4] Kim J, Bae C, Kim G. Simulation on the effect of the combustion parameters on the piston dynamics and engine performance using the Wiebe function in a free piston engine [J]. Applied Energy, 2013, 107(0306-2619): 446-455.

[5] Jia Boru, Zuo Zhengxing, Tian Guohong, et al. Development and validation of a free-piston engine generator numerical model [J]. Energy Conversion & Management, 2015, 91(0196-8904): 333-341.

[6] Jia Boru, Smallbone A, Zuo Zhengxing, et al. Design and simulation of a two- or four-stroke free-piston engine generator for range extender applications [J]. Energy Conversion & Management, 2016, 111: 289-298.

[7] Guo Chendong, Zuo Zhengxing, Jia Boru, et al. Parametric analysis of a dual-piston type free-piston gasoline engine linear generator [J]. Energy Procedia, 2019, 158: 1431-1436.

[8] Mikalsen R, Roskilly A P. Performance simulation of a spark ignited free-piston engine generator [J]. Applied Thermal Engineering, 2008, 28(14-15): 1726-1733.

[9] Li Qingfeng, Xiao Jin, Huang Zhen. Simulation of a two-stroke free-piston engine for electrical power generation [J]. Energy & Fuels, 2008, 22(5): 3443-3449.

[10] Mikalsen R, Roskilly A P. Coupled dynamic–multi-dimensional modelling of free-piston engine combustion [J]. Applied Energy, 2009, 86(1): 89-95.

[11] Mikalsen R, Roskilly A P. A computational study of free-piston diesel engine combustion [J]. Applied Energy, 2009, 86(7-8): 1136-1143.

[12] Xiao Jin, Li Qingfeng, Huang Zhen. Motion characteristic of a free piston linear engine [J]. Applied Energy, 2010, 87(4): 1288-1294.

[13] Xu Shuaiqing, Wang Yang, Zhu Tao, et al. Numerical analysis of two-stroke free piston engine operating on HCCI combustion [J]. Applied Energy, 2011, 88(11): 3712-3725.

[14] Kosaka H, Akita T, Moriya K, et al. Development of free piston engine linear generator system part 1 : Investigation of fundamental characteristics[R]. SAE Technical Papers, 2014, DOI:10.4271/2014-01-1203.

[15] Yuan Chenheng, Feng Huihua, He Yituan, et al. Combustion characteristics analysis of a free-piston engine generator coupling with dynamic and scavenging [J]. Energy, 2016, 102: 637-649.

[16] Zhou Yicong, Sofianopoulos A, Gainey B, et al. A system-level numerical study of a homogeneous charge compression ignition spring-assisted free piston linear alternator with various piston motion profiles [J]. Applied Energy, 2019, 239: 820-835.

[17] Jia Boru. Investigation on the starting and operation processes of a spark-ignited free-piston engine generator [D]. Beijing: Beijing Institute of Technology, 2017. (in Chinese)

[18] Tian Chunlai. Research on dynamics and control strategy of free-piston engine for linear generator[D]. Beijing: Beijing Institute of Technology, 2012. (in Chinese)

[19] Li Long. Research on variable-load control for stable operation of free-piston engine generator[D]. Beijing: Beijing Institute of Technology, 2017. (in Chinese)